Journal of Power Sources 195 (2010) 6860–6866

Contents lists available at ScienceDirect

Journal of Power Sources

journal homepage: www.elsevier.com/locate/jpowsour

Improved electrochemical performance of $AlPO_4$-coated $LiMn_{1.5}Ni_{0.5}O_4$ electrode for lithium-ion batteries

Jin Yi Shi [a,b], Cheol-Woo Yi [c,*], Keon Kim [a,**]

[a] Department of Chemistry, Korea University, Seoul 136-701, South Korea
[b] Jilin Institute of Chemical Technology, Jilin 132022, China
[c] Department of Chemistry and Institute of Basic Science, Sungshin Women's University, 249-1 Dongseon-dong 3-ga, Seoul 136-742, South Korea

ARTICLE INFO

Article history:
Received 5 November 2009
Received in revised form 8 February 2010
Accepted 12 February 2010
Available online 8 April 2010

Keywords:
Lithium-ion battery
Cathode
Surface modification
Coating

ABSTRACT

$LiMn_{1.5}Ni_{0.5}O_4$ materials coated with $AlPO_4$ are prepared by a sol–gel method with citric acid to improve their electrochemical performance; the physical and electrochemical properties are characterized by various analytical techniques. The coated $AlPO_4$ layer completely covers the surfaces of the $LiMn_{1.5}Ni_{0.5}O_4$ particles and the thickness of the coated layer is ~15 nm. 1 wt.% $AlPO_4$-coated $LiMn_{1.5}Ni_{0.5}O_4$ has much lower surface and charge-transfer resistances and shows a higher lithium diffusion rate in comparison with the pristine sample. The modified material demonstrates dramatically enhanced electrochemical reversibility and stability under elevated temperature conditions. This is because the coated $AlPO_4$ layer reduces the contact area between the electrode and electrolyte and suppresses the formation of undesirable solid electrolyte interface films.

1. Introduction

Lithium-ion batteries have become very popular for use as power sources for laptop computers, cell phones, digital cameras, and other portable consumer electronics due to their high specific energy and good cycleability [1]. Currently, $LiCoO_2$, $LiNiO_2$, and $LiMn_2O_4$ cathode materials are used widely in commercial lithium-ion batteries [2–8]. Among them, spinel $LiMn_2O_4$ is considered to be the most promising, due to its various advantages, such as its abundance, low cost, non-toxicity, etc. [9]. Nevertheless, due to the Jahn–Teller effect [10,11] and the dissolution of Mn in the electrolyte [12,13], which result in rapid capacity fading, the practical application of $LiMn_2O_4$ is limited. In order to overcome these obstacles, many investigations have been performed, which proved that the addition of transition metals to the lattice of $LiMn_2O_4$ is an effective way to minimize the Jahn–Teller effect [10,11,14]. Moreover, coating of protective layers on the surface of the $LiMn_2O_4$ particles reduces the dissolution of Mn [5,12,13]. It has recently been reported that $LiMn_{2-x}M_xO_4$ (M = Ni, Cr, Cu, Fe, and Co) has a high voltage plateau at ~5 V and delivers a high capacity in the range of 130–150 mAh g^{-1} [15–19]. In particular, a great deal of attention has been paid to $LiMn_{1.5}Ni_{0.5}O_4$ because of its good cyclic properties and relatively high initial capacity [19,20]. Despite these advantages, this material still undergoes decomposition of electrolyte and dissolution of Mn and Ni, particularly under high voltage and elevated temperature conditions [21–24]. In published work from other groups, coating of ZnO [25], Al_2O_3 [26], and SiO_2 [27] on the active material has been shown to suppress the formation of HF and the dissolution of transition metal ions. Cho et al. [28,29] reported that $LiCoO_2$ cathodes coated with $AlPO_4$ have improved thermal stability and electrochemical performance because, in contrast to other metal oxides (Al_2O_3 and ZrO_2), $AlPO_4$ forms homogeneous surface layers.

In the present study, $AlPO_4$ is employed as a coating material to improve the thermal stability and electrochemical performance of $LiMn_{1.5}Ni_{0.5}O_4$ cathodes. $AlPO_4$-coated $LiMn_{1.5}Ni_{0.5}O_4$ is prepared by a sol–gel method with citric acid. The physical and electrochemical properties of the $AlPO_4$-coated $LiMn_{1.5}Ni_{0.5}O_4$ are investigated by various analytical techniques. $LiMn_{1.5}Ni_{0.5}O_4/AlPO_4$ demonstrates enhanced electrochemical performance in comparison with pristine $LiMn_{1.5}Ni_{0.5}O_4$, even under elevated temperature conditions.

2. Experimental

$LiMn_{1.5}Ni_{0.5}O_4$ was synthesized by a sol–gel method with citric acid. Stoichiometric amounts of $CH_3COOLi{\cdot}2H_2O$ (Aldrich), $Mn(CH_3COO)_2{\cdot}4H_2O$ (Aldrich), $Ni(CH_3COO)_2{\cdot}4H_2O$ (Aldrich), and citric acid (Aldrich) were dissolved in distilled water, and the mole ratio of citric acid to total metal ions was fixed at 1. Ammonium

* Corresponding author. Tel.: +82 2 920 7666; fax: +82 2 920 2047.
** Corresponding author. Tel.: +82 2 953 1172; fax: +82 2 953 1172.
E-mail addresses: cheolwoo@sungshin.ac.kr (C.-W. Yi), kkim@korea.ac.kr (K. Kim).

0378-7753/$ – see front matter © 2010 Elsevier B.V. All rights reserved.
doi:10.1016/j.jpowsour.2010.02.063

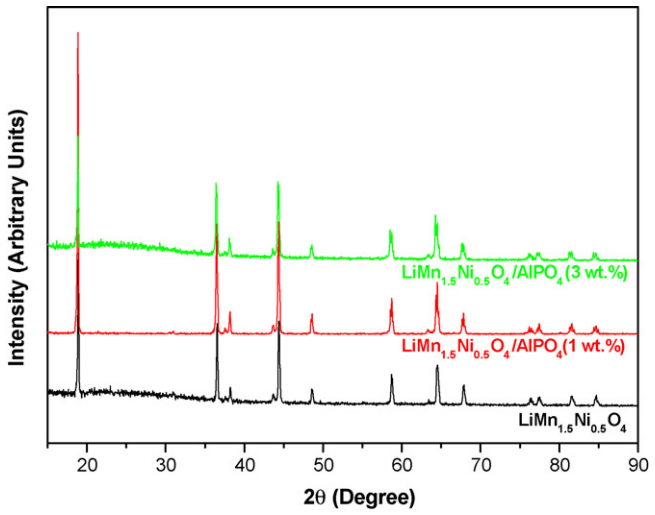

Fig. 1. X-ray diffraction patterns of pristine and modified $LiMn_{1.5}Ni_{0.5}O_4$.

hydroxide was added slowly to the solution until the pH was within the range of 8.0–9.0. Subsequently, the solution was stirred at 80 °C to form a viscous transparent gel, and then the gel was preheated at 500 °C for 3 h to decompose the organic components. The resulting precursor was annealed at 850 °C for 15 h.

To prepare $AlPO_4$ (1 and 3 wt.%)-modified $LiMn_{1.5}Ni_{0.5}O_4$ samples, $Al(NO_3)_3{\cdot}9H_2O$ (Aldrich) and the as-prepared $LiMn_{1.5}Ni_{0.5}O_4$ powder were mixed in distilled water, and then $(NH_4)_2HPO_4$ (Aldrich) solution was slowly dropped into the suspension with stirring. The solvent was evaporated at 80 °C and was followed by a drying process at 120 °C with final annealing at 550 °C for 5 h. Each electrode (cathode) was prepared by mixing 10 mg of the active powder and 4.0 mg of teflonized acetylene black and pressing the mixture to form a 1 cm^2 pellet, which was then dried in a vacuum at 120 °C for 12 h. Lithium metal and polypropylene were used as the anode and separator, respectively. The electrolyte was 1.0 M $LiPF_6$ dissolved in a 1:1 mixture of ethylene carbonate (EC) and dimethylcarbonate (DMC) solution (TECHNO Semichem Co.). Coin-type cells (CR2032) were assembled in an argon-filled glove-box.

The structure of the products was characterized by X-ray diffraction (XRD) using a Rigaku DMAX-III diffractometer equipped with a Cu target. The morphology of the products was examined by field emission-scanning electron microscopy (FE-SEM, Hitachi S-4300) coupled with energy dispersive spectroscopy (EDS, Horiba EX-200). Auger electron spectroscopy (AES, PHI-680) was employed at a sputtering rate of 62 Å min^{-1} to examine the depth profile of the sample composition. Differential scanning calorimetry (DSC) was performed on pristine and $AlPO_4$-coated $LiMn_{1.5}Ni_{0.5}O_4$ samples after charging at 4.95 V for 24 h. The data were acquired using a TA instrument (DSC 2010) in a nitrogen atmosphere at a scan rate of 10 °C min^{-1}. Charge–discharge tests and chronoamperometry (CA) were performed using a WBCS 3000 unit (WonA Tech, Korea). Electrochemical impedance spectroscopy (EIS) was carried out with an IM6 electrochemical instrument (ZAHNER Elektrik, Germany).

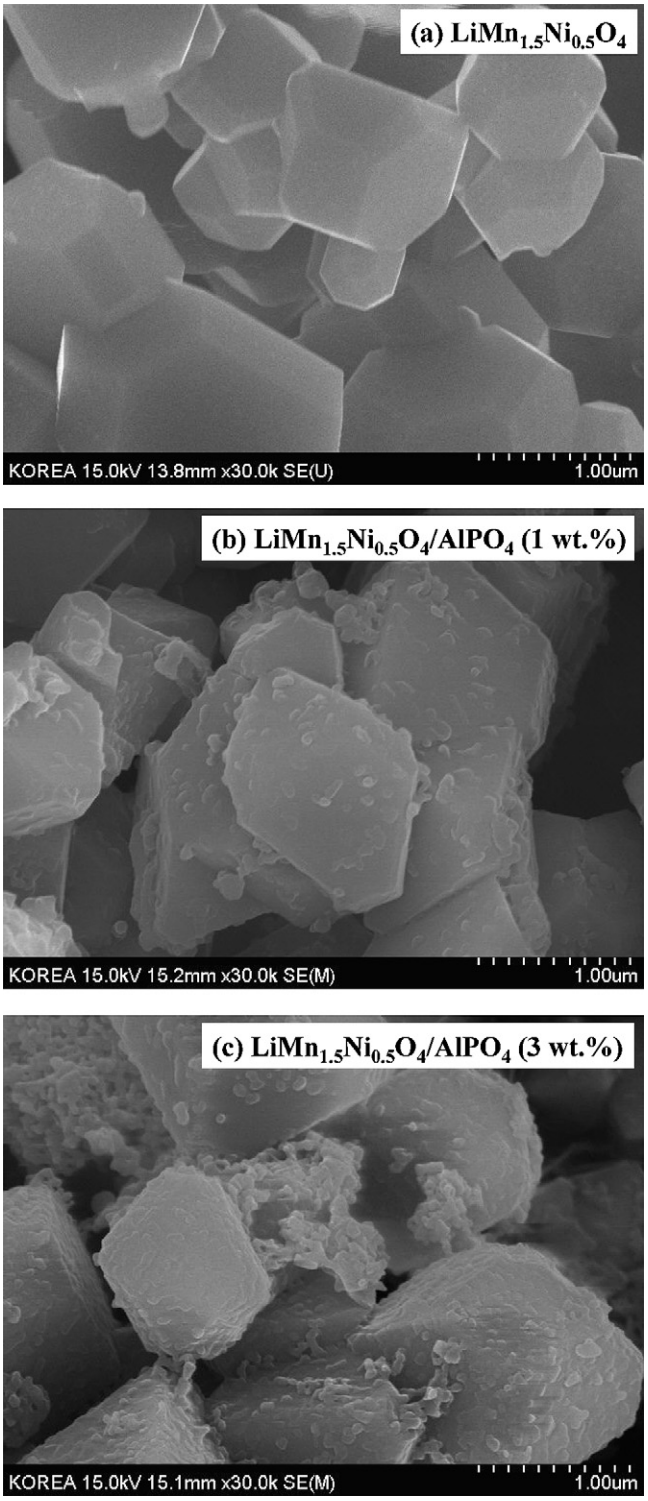

Fig. 2. FE-SEM images of (a) pristine $LiMn_{1.5}Ni_{0.5}O_4$, (b) $LiMn_{1.5}Ni_{0.5}O_4/AlPO_4$ (1 wt.%), and (c) $LiMn_{1.5}Ni_{0.5}O_4/AlPO_4$ (3 wt.%).

3. Results and discussion

The XRD patterns of pristine and modified $LiMn_{1.5}Ni_{0.5}O_4$ prepared by a sol–gel method with citric acid are presented in Fig. 1. The diffraction peaks for the samples are readily indexed to a cubic spinel structure with a minor impurity. The main peaks are sharp, and thus indicate that the samples are well-crystallized. Small impurity features are positioned at 37.5°, 43.7°, and 63.3°; these are assigned to $Li_xNi_{1-x}O$ [19,20,23,27]. Arunkumar and Manthiram [30] have reported that the solubility limit of Ni in $LiMn_{2-x}Ni_xO_4$ is $x < 0.5$ and observed that the impurity phase ($Li_xNi_{1-x}O$) is formed at annealing temperatures above 750 °C when $x = 0.5$. Moreover, the intensity ratio of the (3 1 1) to (4 0 0) peaks of the pristine sample is 0.94, whereas those of the 1 and 3 wt.% $AlPO_4$-coated $LiMn_{1.5}Ni_{0.5}O_4$ samples are 1.00 and 0.99, respectively. It has been reported [17,31,32] that the intensity ratio is related to the stability of the cubic structure, and it is generally accepted that metal-doped

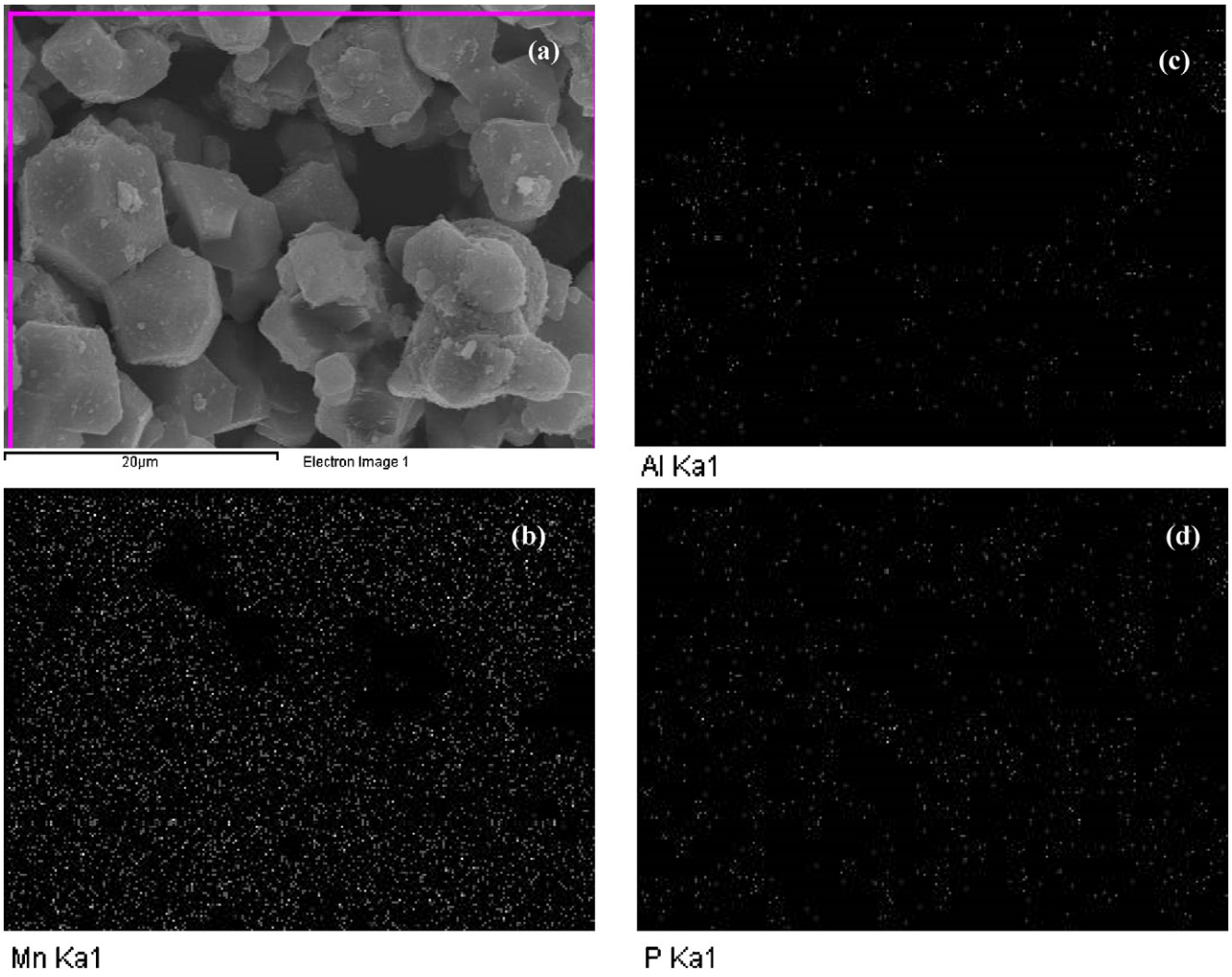

Fig. 3. FE-SEM image (a) and EDS dot-mappings for Mn (b), Al (c), and P (d) of $LiMn_{1.5}Ni_{0.5}O_4/AlPO_4$ (1 wt.%) powder.

$LiMn_2O_4$ compounds with ratios between 0.96 and 1.1 have better electrochemical properties. The X-ray diffraction patterns of the modified samples, however, do not have any diffraction patterns corresponding to $AlPO_4$, due probably to the low concentration of this phase.

Further investigations were performed to characterize the coated layers and investigate the other physical properties of the samples. The SEM images of the pristine and $AlPO_4$-coated $LiMn_{1.5}Ni_{0.5}O_4$ are shown in Fig. 2. The surface morphology of the pristine $LiMn_{1.5}Ni_{0.5}O_4$ is smooth and clean. On the other hand, the surface of the coated $LiMn_{1.5}Ni_{0.5}O_4$ is covered with small particles that consist mainly of $AlPO_4$, as shown in Fig. 2(b) and (c). The compositions of the small particles on the surface were determined by AES analysis. The distribution of Al and P on $LiMn_{1.5}Ni_{0.5}O_4$ was examined by EDS, and the results are displayed in Fig. 3. The dense accumulation of Mn spots in Fig. 3(b) is attributed to the core material of $LiMn_{1.5}Ni_{0.5}O_4$. The elemental map of Al shows a similar intensity distribution to that of P, as shown in Fig. 3(c) and (d). This indicates that Al and P are homogeneously dispersed on the surface of the $LiMn_{1.5}Ni_{0.5}O_4$ particles, since there is no significant agglomeration of these elements. The XRD, SEM, and EDS results suggest the possibility that the surface modification of $LiMn_{1.5}Ni_{0.5}O_4$ with $AlPO_4$ suppresses the decomposition [24] and/or side reaction [22] of the electrolyte at the electrode surface and the dissolution of Mn and Ni ions. This is because the evenly-dispersed $AlPO_4$ on $LiMn_{1.5}Ni_{0.5}O_4$ acts as a protecting layer and reduces the direct contact between the active cathode material and electrolyte.

In order to determine the thickness of the coated layers, an AES experiment was performed. The average atomic concentrations of Al and Mn for 1 wt.% $AlPO_4$-coated $LiMn_{1.5}Ni_{0.5}O_4$ as a function of the depth from the surface are shown in Fig. 4(a). The data clearly show a decrease in the atomic concentration of Al as the depth perpendicular to the surface increases; conversely, the Mn concentration increases. It should be noted, however, that AES does not show the true concentrations of Al and Mn as a function of depth, because the Auger electrons ejected from Al and Mn have different inelastic mean free paths (IMFPs). That is, the concentrations displayed in the depth profile (Fig. 4(a)) are not the true concentrations of the topmost surface, but those including the topmost surface and some layers underneath it. The kinetic energies of the Auger electrons ejected from Al (KLL transition) and Mn (LMM transition) are ~1400 and ~600 eV, and the corresponding IMFPs of the Al and Mn Auger electrons are 27.7 and ~11 Å, respectively [33,34]. This suggests that the initial concentration of aluminium is overestimated because the peak-to-peak intensity of AES is proportional to the IMFP. The data in Fig. 4(b) show that the relative concentration of Al decreases abruptly and its actual concentration drops down to zero at ~15 nm, which is the thickness of the $AlPO_4$ layer. On the other hand, the relative concentration of Mn concomitantly increases and eventually becomes constant.

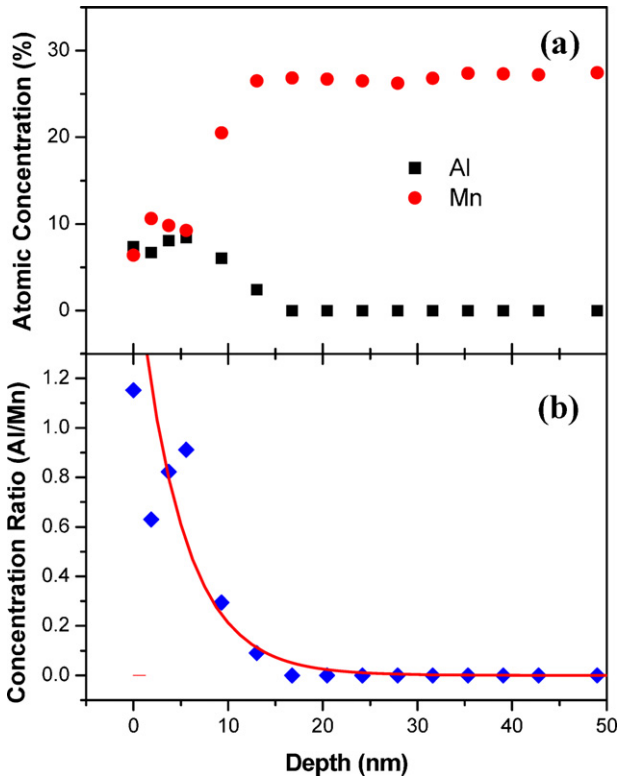

Fig. 4. Auger electron spectroscopy depth profiles of $LiMn_{1.5}Ni_{0.5}O_4/AlPO_4$ (1 wt.%) powder: (a) atomic concentrations of Al and Mn and (b) concentration ratio of Al to Mn as a function of depth from surface.

Table 1
Measured EIS data of pristine and modified $LiMn_{1.5}Ni_{0.5}O_4$ electrodes after 3 cycles.

	$LiMn_{1.5}Ni_{0.5}O_4$	$LiMn_{1.5}Ni_{0.5}O_4/AlPO_4$ (1 wt.%)	$LiMn_{1.5}Ni_{0.5}O_4/AlPO_4$ (3 wt.%)
R_{sol} (Ω)	2.1	2.1	2.0
R_{SEI} (Ω)	5.9	4.3	12.31
R_{CT} (Ω)	52.8	20.7	33.71

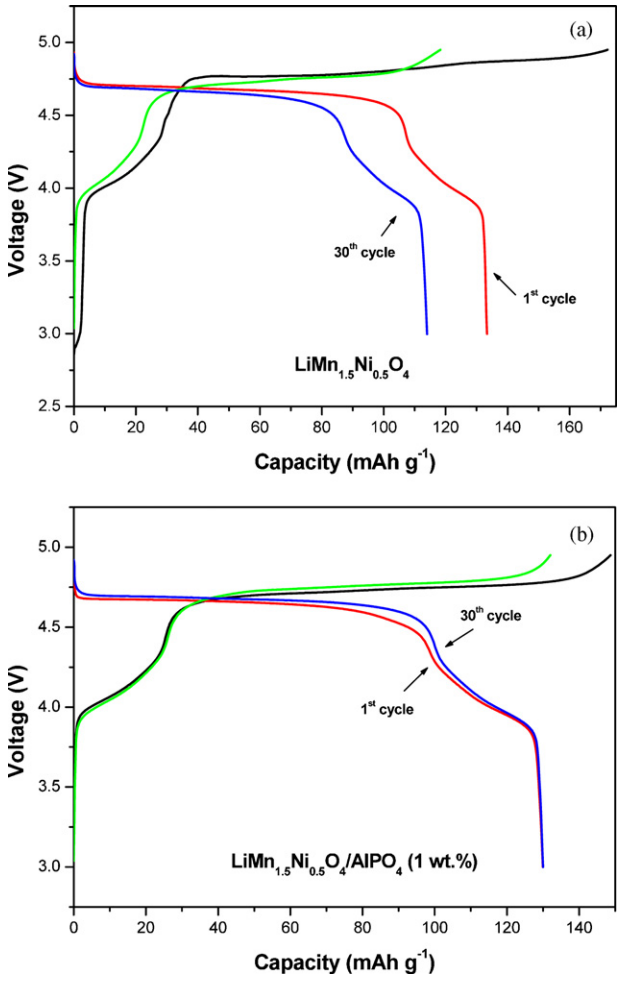

Fig. 5. Charge and discharge curves of (a) pristine $LiMn_{1.5}Ni_{0.5}O_4$ and (b) $LiMn_{1.5}Ni_{0.5}O_4/AlPO_4$ (1 wt.%) at 55 °C in voltage range 3.0–4.95 V.

To study the electrochemical performance of $AlPO_4$-coated $LiMn_{1.5}Ni_{0.5}O_4$, the charge and discharge capacities were measured with different numbers of charge–discharge cycles. The charge and discharge characteristics of the cathode materials, $LiMn_{1.5}Ni_{0.5}O_4$ (Fig. 5(a)) and $LiMn_{1.5}Ni_{0.5}O_4/AlPO_4$ (1 wt.%) (Fig. 5(b)) under elevated temperature conditions are presented in Fig. 5. Two unambiguous plateaux are observed in the case of the pristine and modified samples during the discharge process. This is consistent with the reports of other groups [17,25,27]. The potential plateau at 4.7 V is assigned to the Ni^{4+}/Ni^{2+} reduction reaction, whereas that at 4.0 V corresponds to the reduction of Mn^{4+} to Mn^{3+}. The initial charge and discharge capacities of pristine $LiMn_{1.5}Ni_{0.5}O_4$ are 172 and 133 mAh g^{-1}, while those of 1 wt.% $AlPO_4$-coated $LiMn_{1.5}Ni_{0.5}O_4$ are 148 and 130 mAh g^{-1}, respectively. The coulombic efficiencies for the initial charge and discharge capacities of pristine and modified $LiMn_{1.5}Ni_{0.5}O_4$ are 77.32% and 87.84%, respectively. The higher coulombic efficiency of the $AlPO_4$-coated $LiMn_{1.5}Ni_{0.5}O_4$ probably originates from the fact that the coated layers reduce the side-reactions, such as the decomposition of the electrolyte, and suppress the formation of undesirable solid electrolyte interface (SEI) layers [21–24]. The discharge capacities of the pristine and modified $LiMn_{1.5}Ni_{0.5}O_4$ cathode materials are given in Fig. 6 as a function of the number of charge–discharge cycles at 55 °C. For pristine $LiMn_{1.5}Ni_{0.5}O_4$, the discharge capacity gradually decreases with increasing number of cycles and reached 115 mAh g^{-1} after 30 cycles. The capacity retention ratio of the pristine sample is 86.47%. On the other hand, the modified samples show better cycleability than the pristine sample, and the capacity retention ratios of the 1 and 3 wt.% $AlPO_4$-coated $LiMn_{1.5}Ni_{0.5}O_4$ are 99.23% and 96.75%, respectively. On the other hand, their initial discharge capacities are lower than the highest values observed during cycling. This indicates that the insulating $AlPO_4$ on the $LiMn_{1.5}Ni_{0.5}O_4$ initially hinders the extraction and insertion of lithium ions passing through the interface. With increasing num-

Table 2
Lithium-ion diffusion parameters of pristine and modified $LiMn_{1.5}Ni_{0.5}O_4$ electrodes.

		$LiMn_{1.5}Ni_{0.5}O_4$	$LiMn_{1.5}Ni_{0.5}O_4/AlPO_4$ (1 wt.%)	$LiMn_{1.5}Ni_{0.5}O_4/AlPO_4$ (3 wt.%)
1st cycle	$-(D\pi^2/r^2)$ (10^{-4} s^{-1})	5.98	3.03	2.94
	D (10^{-13} cm^2 s^{-1})	6.06	3.07	2.99
10th cycle	$-(D\pi^2/r^2)$ (10^{-4} s^{-1})	4.59	8.21	5.29
	D (10^{-13} cm^2 s^{-1})	4.65	8.33	5.37

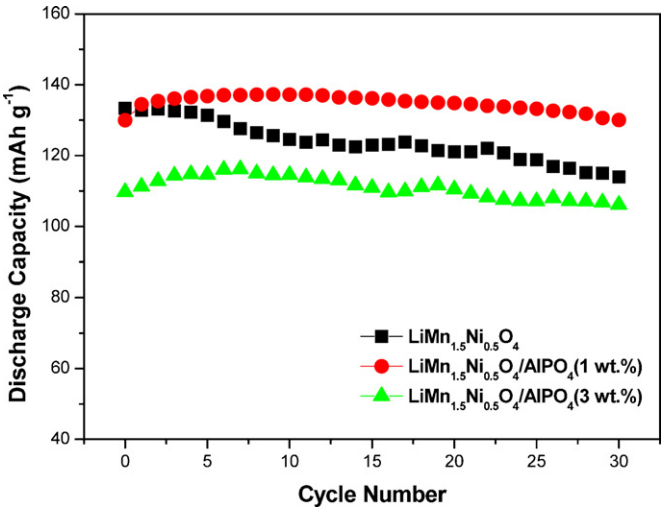

Fig. 6. Cycling behaviour of pristine and modified samples at 55 °C.

ber of cycles, however, the coated layer is probably activated. As a result, lithium ions can easily penetrate through the coated protecting layer and become deeply inserted into the lattice of $LiMn_{1.5}Ni_{0.5}O_4$. To support this finding, EIS and CA were performed using pristine and modified $LiMn_{1.5}Ni_{0.5}O_4$ samples. The results are discussed in detail in the following paragraphs.

The typical impedance spectra of pristine $LiMn_{1.5}Ni_{0.5}O_4$ and $AlPO_4$-coated $LiMn_{1.5}Ni_{0.5}O_4$ electrodes after 3 cycles at 55 °C are presented in Fig. 7; each EIS spectrum presents two overlapped semicircles. Barsoukov and Macdonald [35] reported that the high-frequency semicircle represents the resistance of the SEI film (R_{SEI}) and the medium-frequency semicircle denotes the charge-transfer resistance (R_{CT}). Each parameter was determined by plot fitting with the equivalent circuit shown in the inset of Fig. 7. The EIS results are summarized in Table 1. The electrochemical impedance spectra were obtained after 3 cycles of charging-discharging, since the SEI film is formed during the first few cycles and changes very little during the following cycles [36]. The modified electrode exhibits a much lower charge-transfer resistance in comparison with pristine $LiMn_{1.5}Ni_{0.5}O_4$, while the SEI resistance of $LiMn_{1.5}Ni_{0.5}O_4/AlPO_4$ (3 wt.%) is higher than that of the pristine sample. Because $AlPO_4$ is electrochemically inactive, an excess amount of $AlPO_4$ coated on the surface of $LiMn_{1.5}Ni_{0.5}O_4$ causes an

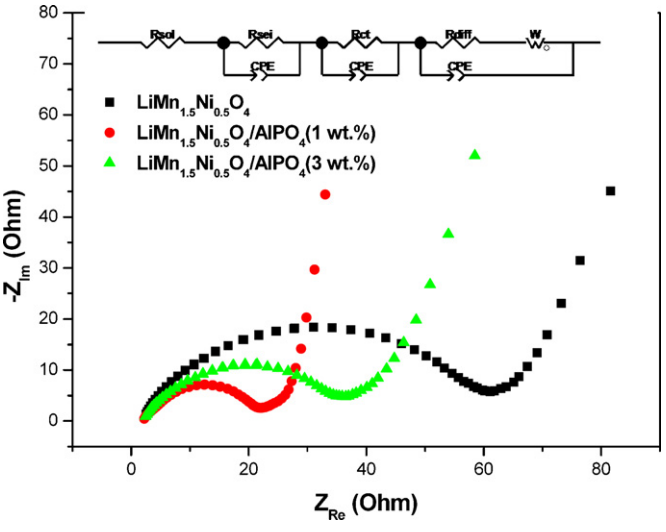

Fig. 7. EIS spectra of pristine and modified $LiMn_{1.5}Ni_{0.5}O_4$ electrodes after 3 cycles.

increase in the SEI resistance. By contrast, the $LiMn_{1.5}Ni_{0.5}O_4/AlPO_4$ (1 wt.%) electrode shows lower surface and charge-transfer resistances (4.3 and 20.7 Ω) than the pristine $LiMn_{1.5}Ni_{0.5}O_4$ electrode (5.9 and 52.8 Ω). These high resistances of the pristine sample are attributed to dissolution of the electrode. Actually, for bare spinel particles without any protecting layer on the surface, the charge and discharge processes in the electrolyte under elevated temperature conditions induce significant dissolution of Mn and/or Ni, and these Mn and/or Ni ions react with the electrolyte to form SEI layers [12,13]. Hence, the dissolution of Mn and/or Ni ions ruins the original surface structure of $LiMn_{1.5}Ni_{0.5}O_4$ and brings about a large increase in the charge-transfer resistance. Therefore, coating an appropriate amount of $AlPO_4$ on $LiMn_{1.5}Ni_{0.5}O_4$ can control the undesirable side-reactions between the electrode and electrolyte and decrease the SEI and charge-transfer resistances. Moreover, the coated layer acts as a buffer layer, which can partially absorb the stress arising from the volume change during cycling, and thereby maintain better contact between the binder, conductive agents and active material [37].

To elucidate the diffusion rate of lithium ions, chronoamperometry was performed on the pristine and modified $LiMn_{1.5}Ni_{0.5}O_4$ cathodes. Fig. 8(a) and (b) shows the diffusion current as a function of diffusion time. For a spherical particle, the diffusion current, i, is expressed by Eq. (1) in the long-time domain ($t \gg r^2/D\pi^2$) [38,39],

$$\ln(-i) = \ln\left(\frac{2nFADC^0}{r}\right) - \left(\frac{D\pi^2}{r^2}\right)t \quad (1)$$

where n is the number of electrons for the charge-transfer reaction; F is the Faraday constant; A is the surface area of the electrode; D is the average diffusion coefficient of lithium ions; C^0 is the concentration of lithium ions of the fully-discharged electrode; r is the radius of the particles composing the electrode; t is the diffusion time. Plots of $\ln(-i)$ as a function of the diffusion time, t, in the range of 2800–3600s are given in Fig. 8(c) and (d). From Eq. (1), the slope is equal to $(-D\pi^2/r^2)$, and the diffusion coefficient (D) can be determined using the particle size obtained from the SEM results. The plot of $\ln(-i)$ versus the diffusion time shows a good linear relationship in the long-time domain, and the average diffusion constant, D, for each of the various electrodes is listed in Table 2. Initially, the modified samples show lower diffusion rates of lithium ions than the pristine sample, due to the inactive $AlPO_4$ layers. After 10 cycles, however, the modified electrode shows an enhanced lithium-ion diffusion rate, because the $AlPO_4$ layer is activated for the transportation of lithium ions. The $LiMn_{1.5}Ni_{0.5}O_4/AlPO_4$ (1 wt.%) electrode shows the highest diffusion rate among the samples. This corresponds to the EIS results, and the fact that the discharge capacity of the first cycle is smaller than the highest value in the cycling test can be explained by the formation of an SEI layer and the activation of the $AlPO_4$ layer.

Differential scanning calorimetry was performed to examine the thermal stability of the delithiated pristine and $AlPO_4$-coated $LiMn_{1.5}Ni_{0.5}O_4$ materials; the results for samples charged at 4.95 V are shown in Fig. 9. The exothermic peak area indicates the amount of heat generated by the decomposition of the cathode. The $AlPO_4$-modified $LiMn_{1.5}Ni_{0.5}O_4$ electrode shows a higher peak temperature (252 °C) and smaller amount of exothermic-heat released in comparison with the pristine electrode. The peak and onset temperatures for the decomposition reaction of delithiated $AlPO_4$-modified $LiMn_{1.5}Ni_{0.5}O_4$ are much higher than those of other delithiated cathode materials, e.g. $LiNiO_2$ (peak temperature: ~200 °C) [40] and $3LaAlO_3$:Al_2O_3-coated $LiCoO_2$ (peak temperature: 185 °C) [41]. It is concluded that the $AlPO_4$-coating improves the thermal stability of the cathode materials, which consequently exhibit lower reactivity with the electrolyte.

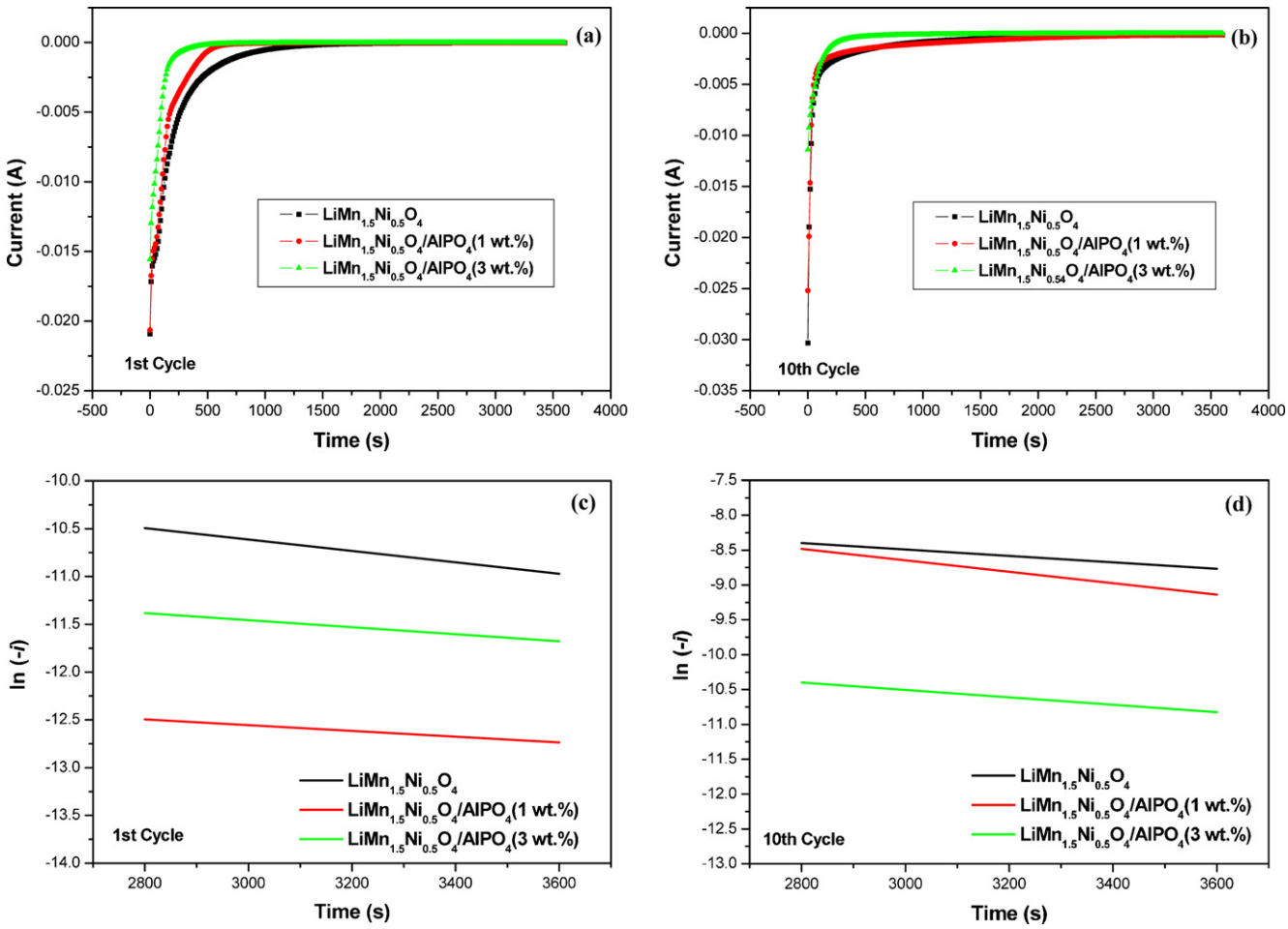

Fig. 8. Chronoamperometry in 1st cycle (a) and 10th cycle (b) and relationship between $\ln(-i)$ and t in 1st cycle (c) and 10th cycle (d) of pristine and modified $LiMn_{1.5}Ni_{0.5}O_4$ electrodes.

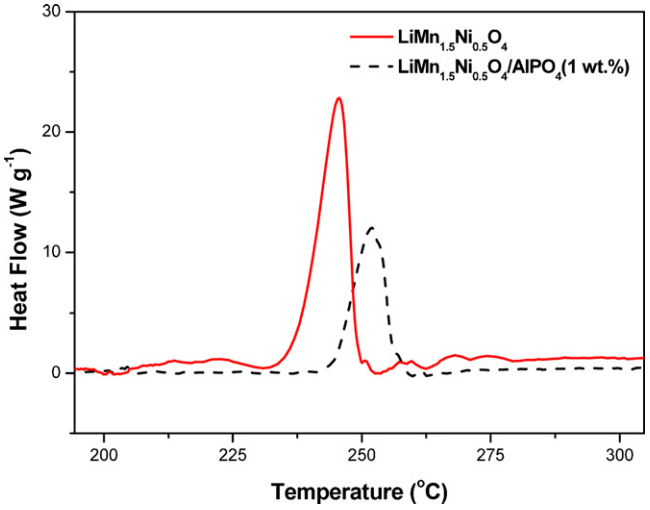

Fig. 9. DSC profiles of pristine and $LiMn_{1.5}Ni_{0.5}O_4/AlPO_4$ (1 wt.%) cells charged at 4.95 V.

4. Conclusions

Surface modified $LiMn_{1.5}Ni_{0.5}O_4$ by $AlPO_4$ has been prepared by a sol–gel method, and its good electrochemical properties and cycle life have been demonstrated. The XRD, SEM-EDS, and AES results indicate that the $AlPO_4$ exists in the form of coated layers on the $LiMn_{1.5}Ni_{0.5}O_4$ particles, rather than interacting with the core material, and that the coated $AlPO_4$ phase completely covers the surface of the particles. The thickness of the coated layers of $LiMn_{1.5}Ni_{0.5}O_4/AlPO_4$ (1 wt.%) is determined to be ~15 nm by AES with sputtering. Moreover, the surface and charge-transfer resistances of the modified electrode (4.3 and 20.7 Ω) are much lower than those of the pristine sample (5.9 and 52.8 Ω), and the lithium diffusion rate of the modified electrode was also significantly enhanced. As a result, the modified materials demonstrate improved electrochemical properties, even under elevated temperature conditions. This improvement is attributed to minimization of the side-reactions between the cathode and electrolyte by the $AlPO_4$ protecting layer, the suppression of the formation of an undesirable SEI layer, and the partial absorption of the stress caused by the volume change during cycling. Therefore, surface modification by $AlPO_4$ is an effective way to improve the performance of $LiMn_{1.5}Ni_{0.5}O_4$ cathode materials for lithium-ion batteries.

Acknowledgements

This work was supported by the ERC program of MOST/KOSEF (Grant No. R11-2002-102-00000-0), as well as by a Sungshin Women's University Research Grant of 2010.

References

[1] J.M. Tarascon, M. Armand, Nature 414 (2001) 359.
[2] W. Li, J.N. Reimers, J.R. Dahn, Phys. Rev. B 46 (1992) 3236.

[3] M. Nishizawa, S. Yamamura, T. Itoh, I. Uchida, Chem. Commun. (1998) 1631.
[4] M.M. Thackeray, W.I.F. David, P.G. Bruce, J.B. Goodenough, Mater. Res. Bull. 18 (1983) 461.
[5] H.W. Ha, N.J. Yun, K. Kim, Electrochim. Acta 52 (2007) 3236.
[6] H.-W. Ha, K.H. Jeong, K. Kim, J. Power Sources 161 (2006) 606.
[7] N.J. Yun, H.-W. Ha, K.H. Jeong, H.-Y. Park, K. Kim, J. Power Sources 160 (2006) 1361.
[8] H.-W. Ha, N.J. Yun, M.H. Kim, M.H. Woo, K. Kim, Electrochim. Acta 51 (2006) 3297.
[9] M.M. Thackeray, P.J. Johnson, L.A. de Picciotto, P.G. Bruce, J.B. Goodenough, Mater. Res. Bull. 19 (1984) 179.
[10] S.R. Das, I.R. Fachini, S.B. Majumder, R.S. Katiyar, J. Power Sources 158 (2006) 518.
[11] E. Wolska, M. Tovar, B. Andrzejewski, W. Nowicki, J. Darul, P. Piszora, M. Knapp, Solid State Sci. 8 (2006) 31.
[12] X. Wang, Y. Yagi, Y.S. Lee, M. Yoshio, Y. Xia, T. Sakai, J. Power Sources 97–98 (2001) 427.
[13] Y. Xia, Y. Zhou, M. Yoshio, J. Electrochem. Soc. 144 (1997) 2593.
[14] K.H. Jeong, H.-W. Ha, N.J. Yun, M.Z. Hong, K. Kim, Electrochim. Acta 50 (2005) 5349.
[15] T. Nakamura, H. Demidzu, Y. Yamada, J. Phys. Chem. Solids 69 (2008) 2349.
[16] S.a. Patoux, L. Sannier, H.e. Lignier, Y. Reynier, C. Bourbon, S.e. Jouanneau, F.i. Le Cras, S.a. Martinet, Electrochim. Acta 53 (2008) 4137.
[17] T.-F. Yi, Y.-R. Zhu, Electrochim. Acta 53 (2008) 3120.
[18] W.K. Zhang, C. Wang, H. Huang, Y.P. Gan, H.M. Wu, J.P. Tu, J. Alloys Compd. 465 (2008) 250.
[19] Q. Zhong, A. Bonakdarpour, M. Zhang, Y. Gao, J.R. Dahn, J. Electrochem. Soc. 144 (1997) 205.
[20] S.H. Oh, S.H. Jeon, W.I. Cho, C.S. Kim, B.W. Cho, J. Alloys Compd. 452 (2008) 389.
[21] Y. Ein-Eli, J.W.F. Howard, J. Electrochem. Soc. 144 (1997) L205.
[22] C. Sigala, A.L.G. La Salle, Y. Piffard, D. Guyomard, J. Electrochem. Soc. 148 (2001) A812.
[23] Y.K. Sun, C.S. Yoon, I.H. Oh, Electrochim. Acta 48 (2003) 503.
[24] Y. Wei, K.-B. Kim, G. Chen, Electrochim. Acta 51 (2006) 3365.
[25] R. Alcantara, M. Jaraba, P. Lavela, J.L. Tirado, J. Electroanal. Chem. 566 (2004) 187.
[26] A. Eftekhari, Chem. Lett. 33 (2004) 616.
[27] Y. Fan, J. Wang, Z. Tang, W. He, J. Zhang, Electrochim. Acta 52 (2007) 3870.
[28] J. Cho, Electrochim. Acta 48 (2003) 2807.
[29] J. Cho, Y.-W. Kim, B. Kim, J.-G. Lee, B. Park, Angew. Chem. Int. Ed. 42 (2003) 1618.
[30] T.A. Arunkumar, A. Manthiram, Electrochim. Acta 50 (2005) 5568.
[31] Y.-S. Lee, N. Kumada, M. Yoshio, J. Power Sources 96 (2001) 376.
[32] Y. Wei, K.W. Nam, K.B. Kim, G. Chen, Solid State Ionics 177 (2006) 29.
[33] S. Tanuma, C.J. Powell, D.R. Penn, Surf. Interface Anal. 11 (1988) 577.
[34] C.W. Yi, J. Szanyi, J. Phys. Chem. C 111 (2007) 17597.
[35] E. Barsoukov, J.R. Macdonald, Impedance Spectroscopy: Theory, Experiment, and Applications, 2nd ed., Wiley-Interscience, 2005.
[36] G. Li, Z. Yang, W. Yang, J. Power Sources 183 (2008) 741.
[37] D. Li, Y. Kato, K. Kobayakawa, H. Noguchi, Y. Sato, J. Power Sources 160 (2006) 1342.
[38] J. Liu, A. Manthiram, J. Phys. Chem. C 113 (2009) 15073.
[39] A. Lundqvist, G. Lindbergh, J. Electrochem. Soc. 145 (1998) 3740.
[40] P. Biensan, B. Simon, J.P. Peres, A. de Guibert, M. Broussely, J.M. Bodet, F. Perton, J. Power Sources 81–82 (1999) 906.
[41] C.-Z. Lu, J.-M. Chen, Y.-D. Cho, W.-H. Hsu, P. Muralidharan, G.T.-K. Fey, J. Power Sources 184 (2008) 392.